Trends in Integration for Magnetically Levitated Pump Systems

T. Nussbaumer, K. Raggl*, P. Boesch, J.W. Kolar*

Levitronix GmbH
Technoparkstrasse 1, 8005 Zurich, Switzerland
nussbaumer@levitronix.com

*Power Electronics Systems Laboratory, ETH Zurich
Physikstrasse 3, 8092 Zurich, Switzerland
kolar@lem.ee.ethz.ch

Abstract– Highly compact magnetically levitated pump systems are of growing interest in semiconductor processing applications due to the increasing costs of clean room space. The need of a higher hydraulic pressure in a smaller mounting volume raises the necessity of a complete integration of the power and signal electronics together with the motor and the pump into one compact system. Thereby, the system complexity is increased in the first instance and problematic issues such as thermal interaction between the system parts and overheating have to be solved. However, the integration opens the door for an optimization of the complete system. Based on a thermal model and on analytical relations between the hydraulic, electric and mechanical system variables the integrated pump system is optimized aiming for maximum pressure density. Exemplarily, the optimum point is calculated for an existing magnetically levitated pump and the dependency of the hydraulic efficiency is discussed.

I Introduction

Due to the necessity of permanent productivity increase in industrial processes also the requirements for pump systems are growing constantly. Especially in the semiconductor industry, where pump systems are utilized for various processes such as cleaning, polishing, etching, etc., particularly the volume and the process quality of the employed systems are crucial productivity parameters. Roadmaps demonstrating the trends in clean room technology point out that the clean room floor space for semiconductor processing has to be reduced to about 50% within the next 3 years. At the same time, the hydraulic pressure will have to be doubled in order to compensate for the pressure losses of improved filter technologies, which are required for future high purity applications.

During the last years, pressure density (i.e. hydraulic pressure per volume) and process quality could be improved significantly by the application of magnetically levitated pump systems [1]-[4], where the im-

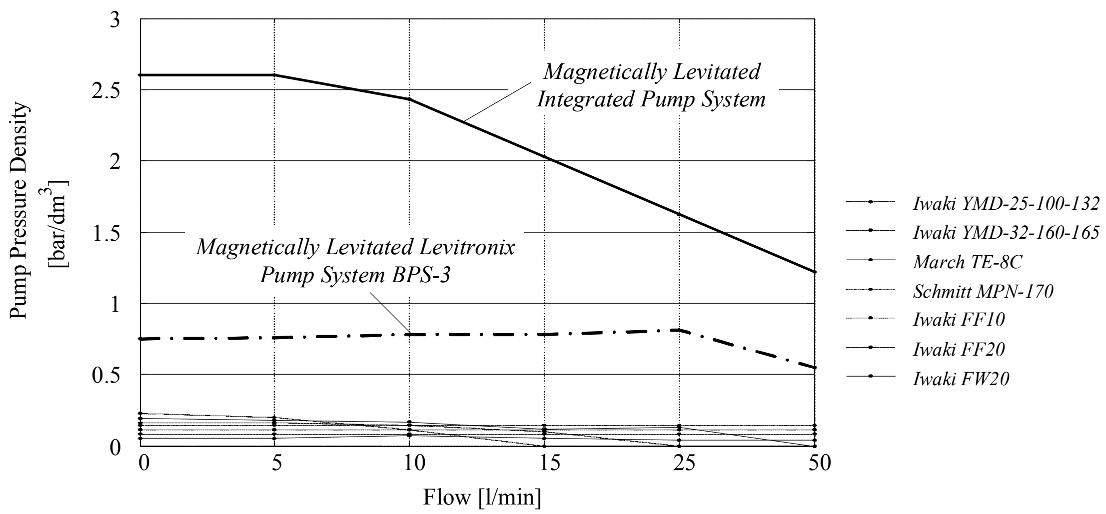

Fig. 1. Comparison of pressure density of different pump technologies for semiconductor applications that deliver a hydraulic pressure between 2 and 4 bar. For the calculation of the total system volume the power and signal electronics is included. On the bottom the pressure density of several commercially available pumps (that are working without the technology of magnetic levitation) are depicted. The upper (solid) curve indicates the expected performance of a fully integrated magnetically levitated pump system.

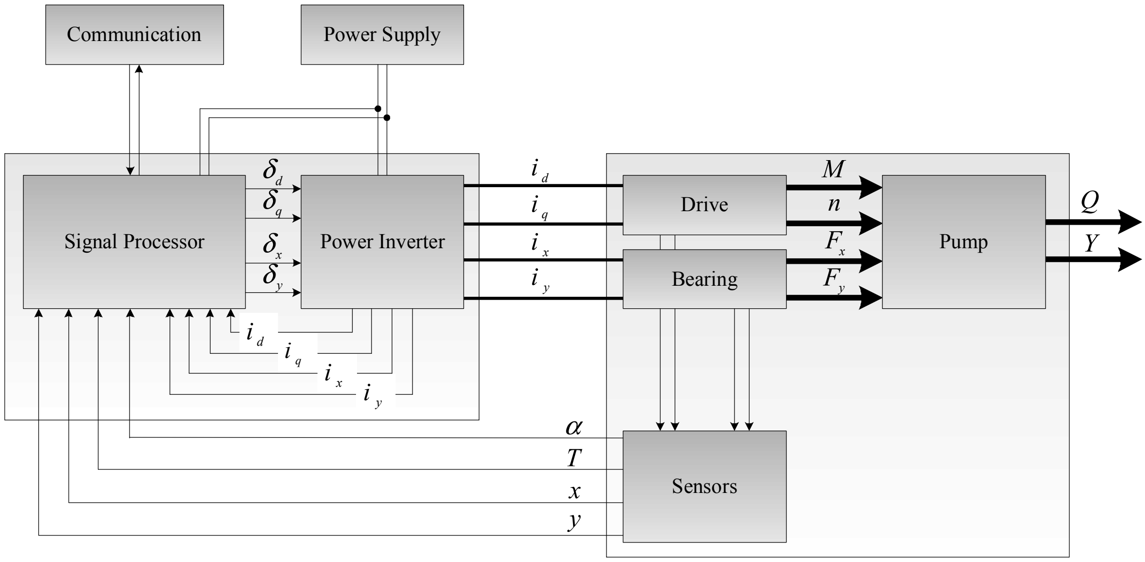

Fig. 2. Setup of a magnetically levitated pump system.

peller is held in position and rotated by magnetic forces. Apart from the fact that these pumps are the best selection in high purity applications due to their lack of bearings, seals and lubricants, they also allow considerably higher pressure ratings in the whole range of flow rates. The predominance of these pumps is shown in **Fig. 1**, where pumps based on the principle of magnetic levitation are compared to commercially available pump systems with magnetically coupled pumps and pneumatic drive bellow pumps.

The characteristic value that is used here for comparison is the hydraulic pressure per volume (i.e. pressure density), which the pumps can provide at certain flow rates. With this, the pressure/flow-curves that are characterizing the pumps are set in relation to their volume including the required power electronics.

For pumps in the semiconductor process industry, the hydraulic pump power would not represent a relevant parameter, since high power can be achieved by high flow rates and moderate hydraulic pressure, which is not required for these applications. Usually, pumps with high hydraulic pressure and low volume at moderate flow rates are demanded. Therefore, the pressure density is a suitable parameter to characterize the pump performance.

However, it has to be noted that the pressure density is not a scalable parameter, since the hydraulic pressure of a pump does not scale with its volume (as shown in section III it scales with d^2, where d is a characteristic length parameter). Therefore, the pressure density only represents a meaningful parameter for the characterization of pumps within a certain pressure range.

In Fig. 1, the performance comparison of the pump systems is shown for the 2-4 bar pressure range which is most relevant for future semiconductor processes. The lower lines indicate the maximum pressure density that can be achieved at the moment by pumps that are working without magnetic levitation for certain flow rates in the range up to 50 l/min [5]-[7]. The selected pumps are already the best-in-class products. However, it can be seen that the magnetically levitated pumps [8] (dashed line) are clearly superior in the whole flow rate range. The solid curve denotes the expected pressure density that can be achieved by integration of the magnetically levitated pumps (the data is drawn from the optimization process described in section IV for realistically achievable hydraulic conditions).

Therefore, the future development has to aim at the integration of the electronics, sensors, motor and pump into one ultra-high compact system. In section II, the route of integration – from modular to full integration – is described and it will be discussed how this leads to a significant volume reduction. Subsequently, the second way to achieve higher pressure density – by means of pressure increase – is analyzed in section III for an existing magnetically levitated pump system. Finally, an optimization procedure is presented in section IV for a future design of a fully integrated pump system with high pressure density and is discussed in section V.

II Volume Reduction – The Route of Integration

Fig. 2 shows the block diagram of a magnetically levitated pump system. The pump which shall provide a specified hydraulic pressure Y at a certain flow

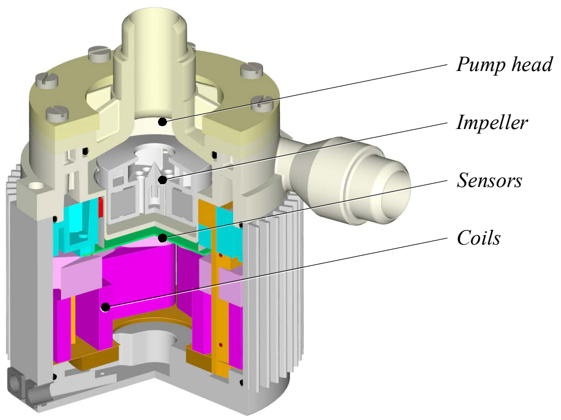

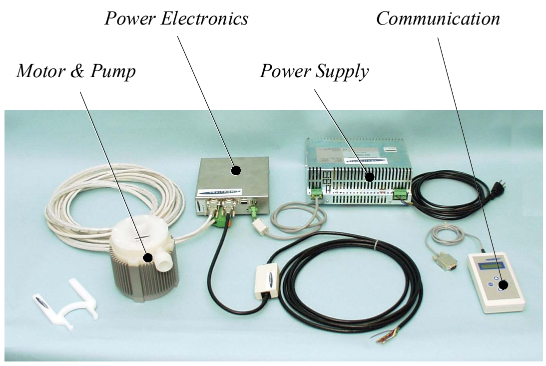

Fig. 3. Structure of the bearingless pump Levitronix BPS-3 (left); required material of the complete pump system (right).

rate Q is driven by a motor that induces the required torque M and rotation speed n. The currents i_d and i_q (for field-oriented control) that are needed for the rotation are impressed into the drive windings by the power inverter. The magnetic forces F_x and F_y that hold the impeller in a desired position are generated and actively controlled by currents i_x and i_y impressed into bearing windings. All currents are controlled in a signal processor which outputs the according PWM duty cycles for the power inverter. In order to calculate the desired reference values for the current controllers, the rotor angle α and the radial positions x and y have to be measured. Additionally, the motor temperature T is measured.

In a conventional setup, these functional blocks are realized as modules with separate casing and cabling in between. Of course, this leads to a big volume of the whole setup that can be optimized by means of integration. The separate blocks are shown in **Fig. 3** (right) along with a detailed view of the bearingless pump (left) [8].

The first level of integration is the arrangement of the power electronics (signal processor and power inverter unit) and the motor and pump as separate working units into one casing with compact design and minimized cabling distances.

Thereby, the space inside the case can be used more efficiently and the cabling effort is reduced significantly. However, the power electronics and the motor and pump are still separate modules of the system. This fact is schematically depicted in **Fig. 4** ("Pump System with Embedded Power Electronics").

Obviously, the cooling surface is reduced in this case and therefore the configuration has to be analyzed and designed also from a thermal point of view. The design in Fig. 4 shows a configuration, where the electronics is stacked directly onto the pump body radially which has a number of advantages as compared to an axial positioning of the electronics:

- The electronics unit serves as the base plate, therefore the pump outlet is positioned vertically. In this

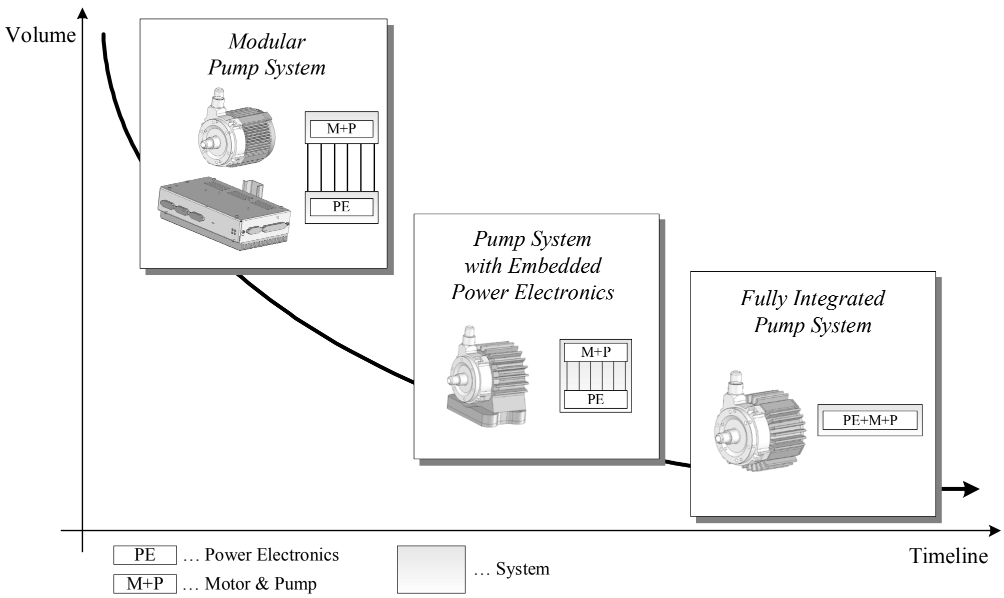

Fig. 4. Levels of integration of the magnetically levitated pump system.

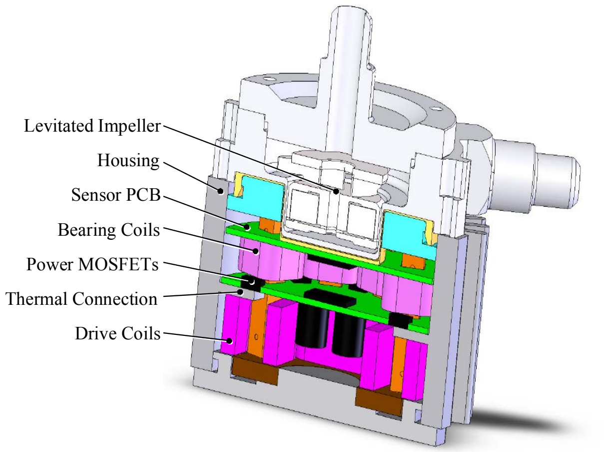

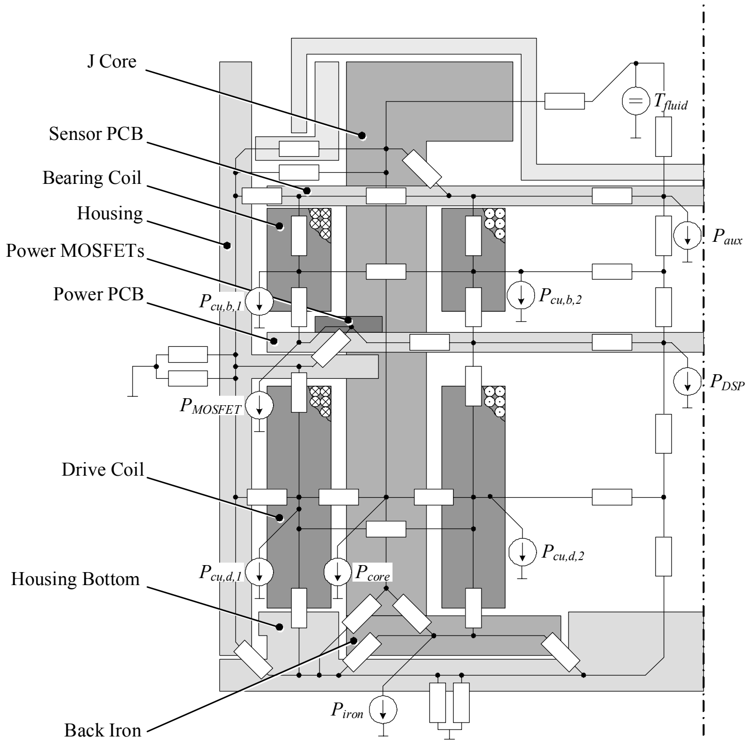

Fig. 5. Sectional view (left) and thermal model (right) of the fully integrated pump system.

configuration eventually occurring bubbles can flow off naturally.

- The motor center (which is a free space in case of the magnetically levitated pump) is accessible from the backside of the pump for the radial configuration and can be used for hydrodynamic balancing or water cooling. For the axial version this access would be blocked up by the electronics.

- An additional module for forced air cooling can be stacked easily onto the back side of the pump without changing the case design. However, for purely natural convection the axial position is advantageous due to the vertical direction of the natural air flow.

Therefore, a radially stacked electronics unit onto the pump case is clearly preferable. The step from modular pump systems to pump systems with integrated power electronics effectuates a considerable volume decrease due to the lack of cabling and casing, which also represents a significant cost portion.

A further step of integration is the full integration, where electronics, motor and pump constitute one system, i.e. the electronics is integrated completely into the motor ("Fully Integrated Pump System" in Fig. 4). Since the cooling surface is further decreased in that case, the before-mentioned thermal aspects are even more problematic in that case. Also, the complexity of the system increases noticeably and the replacement of electronics modules is not possible anymore.

Therefore, in the first instance, problems associated with the full integration seem to outweigh the advantage of volume reduction. However, only a full integration allows an overall optimization of the pump system (as shown later in section IV) aiming for ultra-high pressure density. Hence, future pump systems will have to be based on that concept, and the associated technical challenges will have to be solved. A possible design of a fully integrated pump system is shown in **Fig. 5** (left).

As mentioned before, particular attention has to be paid to a scalable thermal design [9]-[11] of the system. By means of equivalent model parameters such as power dissipation sources [W], temperatures [K] and thermal resistances R_{th} [K/W] the thermal stresses of all components of the pump system can be calculated. This serves as a basis for the system design, e.g. the positioning of the power and signal electronics layers, the selection of the isolation dimensions and materials, and the constructive design of the heat sink. In Fig. 5 (right) the thermal model of a possible setup of an integrated pump system is shown with the appropriate power loss sources, temperatures and thermal resistances.

The thermal model has to be included in an optimization of the fully integrated pump system as done in section IV, where pressure density is maximized under consideration of thermal constraints.

III Pressure Increase

The second way to raise the pressure density of the system is by means of direct increase of the hydraulic pressure. Basically, for an existing pump system, where the pump, motor and electronics outer dimensions are not changed, this can be done by two ways [13]-[18]:

- larger impeller diameter d_i

- higher rotation speed n.

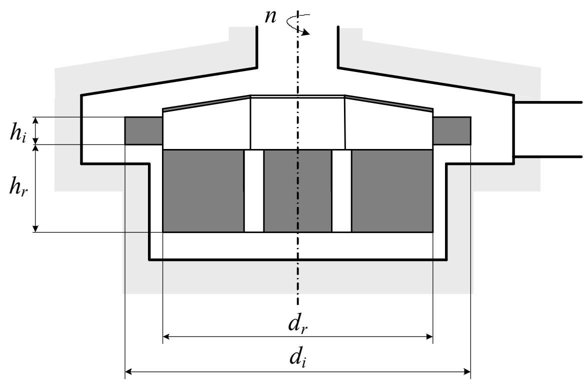

Fig. 6: Schematic view of the pump head.

However, as will be shown in the following, the consequences in terms of power losses are quite different. If the impeller diameter (cf. **Fig. 6**) and/or the rotation speed are enlarged, the hydraulic pressure Y increases quadratically with both parameters

$$Y_1 \sim d_i^2 \cdot n^2 . \tag{1}$$

If the load is changed in such a manner that the flow rate Q keeps constant (which is important to perform a fair comparison) due to

$$P_{hyd} = Y \cdot Q \tag{2}$$

the hydraulic power [11],[13] also increases quadratically

$$P_{hyd} \sim d_i^2 \cdot n^2 . \tag{3}$$

Therefore, the increase of impeller diameter and rotation speed has the same effect on hydraulic pressure and power. However, with

$$\frac{P_{hyd}}{\eta_{hyd}} = P_{mot} = M \cdot \omega \sim I_{Drive} \cdot n \tag{4}$$

the required motor torque M and the drive current I_{Drive}, respectively, are increasing linearly with n and quadratically with d_i:

$$M \sim I_{Drive} \sim n \cdot d_i^2 . \tag{5}$$

Hence, the copper losses [3] are increased by

$$P_{Cu} = R_{Cu} \cdot I_{Drive}^2 \sim n^2 \cdot d_i^4 . \tag{6}$$

On the other hand, the iron losses [19]-[21] mainly have a square dependency (the linear term is usually smaller) only on the rotation speed

$$P_{Fe} \sim n^2 . \tag{7}$$

Fig. 7 shows the compilation of the normalized loss portions with dependency on the impeller diameter and on the rotation speed based on the Eqs. (1)-(7) and an existing pump system. For a well-balanced design, usually iron losses and copper losses show reasonably similar values, wherefore the pressure increase by impeller diameter enlargement leads for higher ratios (≥ factor 1.5) to clearly higher total losses than due to a rotation speed increase.

Of course, the higher torque according to (5) would require an increased motor size, which is not desired. An interesting solution is to increase the rotation speed and decrease the impeller diameter such that the electric torque (and therefore the motor size and the copper losses) remain constant, while the hydraulic pressure and power would scale with n according to (1) and (3). However, since the iron losses still increase with n^2 [cf. (7)], for higher rotation speeds preferably laminated cores should be employed.

Therefore, a pressure increase for an existing pump system (keeping the same motor dimensions) leads to larger rotation speed and smaller impeller size.

IV Optimization of the Integrated Pump System

In the previous section, measures for a pressure density increase have been discussed for existing pump and motor configurations based on physical relations. This was done without changing the pump and motor design and/or dimensions. However, for an optimized

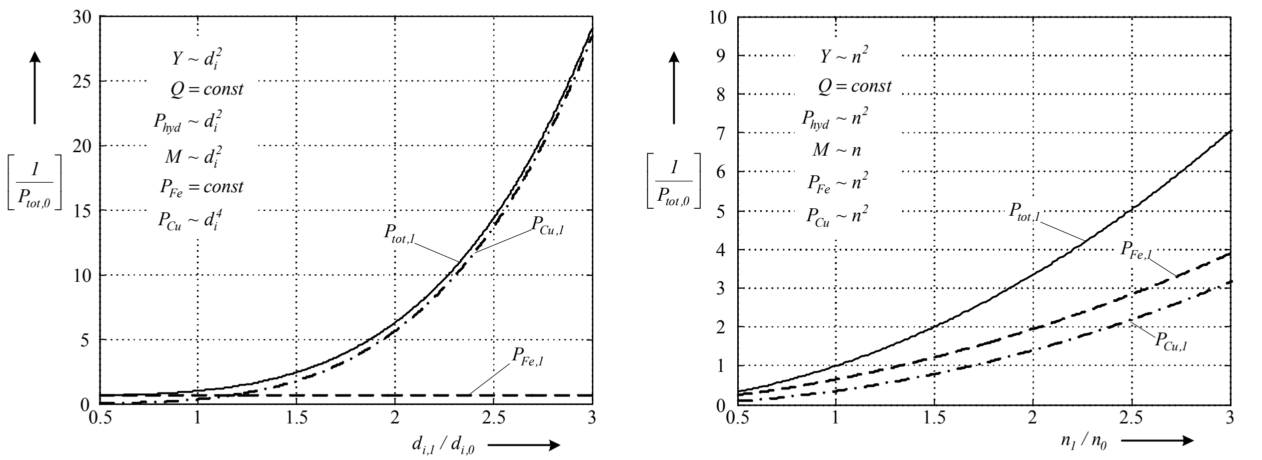

Fig. 7: Normalized power losses for an existing magnetically levitated pump for constant flow rate and for a change of the impeller diameter d_i (a); for a change of the rotation speed n (b). The index 0 denotes the actual values and the index 1 represents the changed parameters.

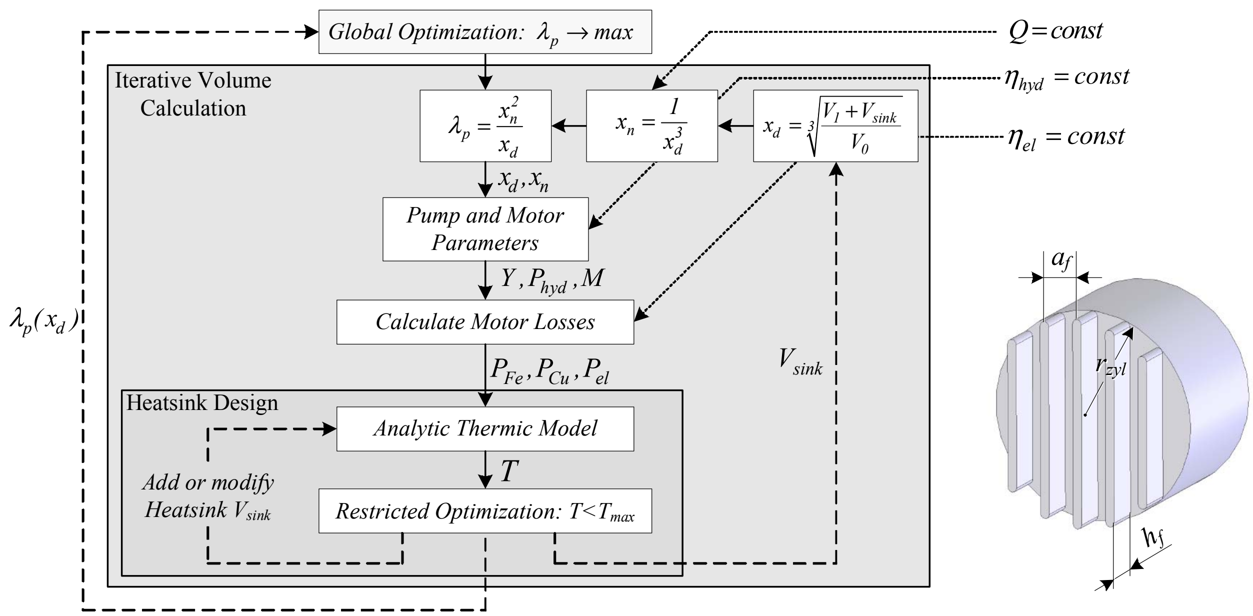

Fig. 8: Optimization Procedure (left); definition of the heat sink dimensions (right).

integrated pump system a complete iterative design procedure as depicted in **Fig. 8** has to be applied. This will be discussed in the following.

Here, the pressure density

$$\lambda_P = \frac{Y}{V} \to \max \tag{8}$$

is maximized by variation of the relative change of all length quantities in the pump system

$$x_d = \frac{d_1}{d_0} = \sqrt[3]{\frac{V_1}{V_0}}, \tag{9}$$

where the index 0 is used for the actual values and the index 1 for the length values in the new (optimized) system. It is assumed that all length quantities (such as case dimensions, impeller diameter, electronics size, coil winding diameter etc..) are changed with that factor in order to scale the whole pump system entirely in a fair manner. For keeping a constant flow rate

$$Q \sim x_n \cdot x_d^3 \tag{10}$$

(which represents a reasonable side condition for the optimization) the relative rotation speed

$$x_n = \frac{n_1}{n_0} \tag{11}$$

has to change according to

$$x_n = \frac{1}{x_d^3}. \tag{12}$$

With this, new values for the pump and motor parameters such as the hydraulic pressure

$$Y_1 = x_d^2 \cdot x_n^2 \cdot Y_0, \tag{13}$$

the hydraulic power

$$P_{hyd,1} = x_d^5 \cdot x_n^3 \cdot P_{hyd,0}, \tag{14}$$

and (under the assumption of a constant hydraulic efficiency) the required motor torque

$$M_1 = x_d^5 \cdot x_n^2 \cdot M_0 \tag{15}$$

can be calculated based on x_d, x_n and the initial values.

Furthermore, based on the resulting motor losses and the thermal model (as discussed in section II) the temperature distribution within the pump system is ascertained. If a local temperature exceeds the allowed local maximum temperature the heat sink is enlarged in an underlying optimization routine. For sake of simplicity the heat sink can be assumed to be stacked on the housing bottom of the pump body (cf. Fig. 8 (right)) and natural convection is assumed. In that case, the optimization variable is the fin height h_f and the fin distance a_f is kept at an optimum value for natural convection.

Obviously, with the additional heat sink volume V_{sink} the total pump volume is increased. Hence, the relative length parameter x_d is not given anymore by Eq. (9) but increased according to

$$x_d = \sqrt[3]{\frac{V_1 + V_{sink}}{V_0}}, \tag{16}$$

wherefore the pressure density is lowered.

This leads to a closed optimization procedure maximizing the pressure density. In the following section, the results of this procedure are illustrated by an exemplary design and discussed.

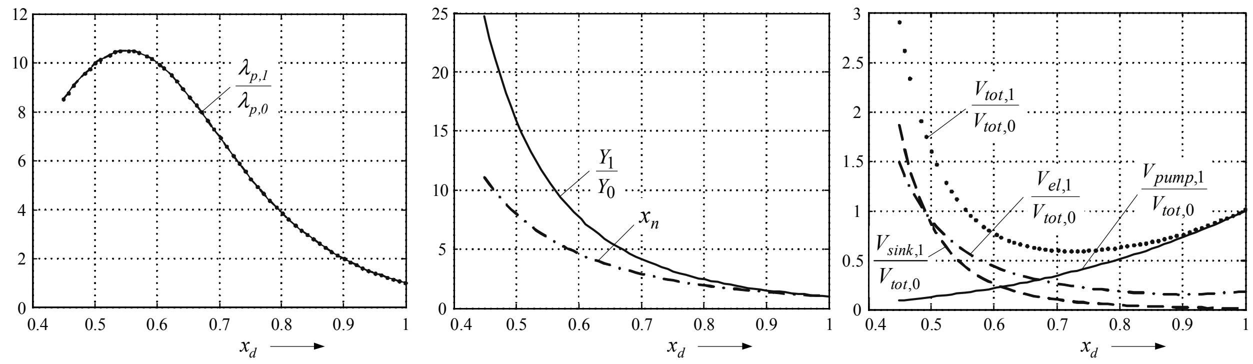

Fig. 9: Results of the optimization procedure (cf. Fig. 8) for an existing magnetically levitated pump (V_0 = 0.9 dm^3, n_0 = 8'000 rpm, Y_0 = 0.8 bar) for constant flow rate Q = 5 l/min and under the assumption of constant hydraulic efficiency and natural convection.

V Discussion

In order to illustrate the procedure, exemplarily an existing integrated pump system with a total volume of V_0 = 0.9 dm^3 shall be optimized. As an operating point a rotation speed of n_0 = 8'000 rpm, a hydraulic pressure of Y_0 = 0.8 bar and a constant flow rate of Q = 5 l/min has been chosen. This pump shall now be pushed towards higher pressure density through the above design procedure.

In **Fig. 9** the curves for the relative change of the pressure density (a), the rotation speed and the hydraulic pressure (b), and the loss portions (c) with reference to the original pump system are plotted. It can be seen that for a relative length change of x_d = 0.55 the pressure density reaches its theoretical maximum and is increased by a factor of 10.5. This is realized by a significant pressure increase up to Y_1 = 8.8 bar (factor 11) while keeping the same total volume as for the beginning. However, in order to reach this point a rotation speed of n_1 = 48'000 rpm (factor 6), is required.

This theoretic optimum point will be hard to achieve because of two reasons. First, for these high rotation speeds the rotor tends to get axially unstable due to the pressure increase, since the axial position is only controlled passively. And secondly, in the presented optimization routine the hydraulic efficiency is assumed to be constant, i.e. the impeller is assumed to be designed specifically for the operating point of interest.

Generally, the hydraulic losses scale in the same manner as the hydraulic power by

$$P_{L,hyd,1} = x_d^5 \cdot x_n^3 \cdot P_{L,hyd,0}, \qquad (17)$$

wherefore the hydraulic efficiency remains approximately constant. However, for very high rotation speeds additional loss terms as e.g. rotor pulsation losses will occur, which will decrease the efficiency to a certain degree. This influence is depicted in **Fig. 10**, where it is shown to which extent the achieved pressure density increase is altered by different hydraulic efficiency values.

In the case at hand, a realistic maximum rotation speed is n_1 = 20'000 rpm, which means a length reduction by a factor of x_d = 0.75 and would effect a hydraulic pressure of 2.4 bar and a pressure density increase by a factor of 5 (cf. Fig. 9). The volume is reduced to V_1 = 0.54 l, which is a factor of 0.6.

Even if the rotation speed increase would reduce the hydraulic efficiency to 50% of the value at 8'000 rpm (which is a worst case assumption) this would still represent a pressure density increase of a factor 4 (cf. Fig. 10).

Until now, the optimization procedure has been based on cooling by natural convection. In a similar manner, forced convection could be included in the optimization procedure, which could lead for high-speed pumps to possibly even more compact designs. Moreover, water-cooled pump systems could allow a further pressure density increase, where, however, the effort for the water cooling has to be considered, too.

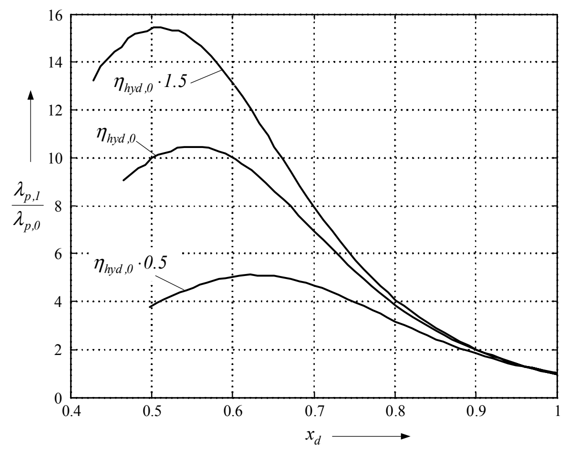

Fig. 10: Influence of the hydraulic efficiency on the pressure density increase that is achieved through the optimization procedure.

VI Conclusions

For pump applications in clean room technology, magnetically levitated pumps already represent the best solution concerning hydraulic pressure per volume. However, for the forthcoming pump generation the total volume of the pump system has to further decrease while at the same time the hydraulic pressure has to increase.

As shown in this paper, this necessarily requires the full integration of the electronics, sensors, motor and pump into one pump unit. This enables an overall optimization of the whole system considering hydraulic, electric, mechanical, and thermal relations. Meanwhile, the hydraulic efficiency is assumed to be constant in the model, wherefore a future step is to completely include the hydraulic design (e.g. impeller design enabling higher rotation speeds) in the optimization routine.

As has been shown, a future magnetically levitated, fully integrated pump generation can realistically achieve a pressure density increase of factor 4, which would permit to achieve the intended productivity improvement in clean room technology.

References

[1] J. Bichsel, "The bearingless electrical machine", *International Symposium on Magnetic Suspension Technology*, vol. 2, Aug. 19-23, 1991, pp. 516-573.

[2] G. Schweitzer, "Active magnetic bearings – chances and limitations", *6th International Conference on Rotor Dynamics*, Oct. 2002, Sydney, Australia, pp. 1-14.

[3] N. Barletta, "Der lagerlose Scheibenläufer", Ph.D. Dissertation, Electrical Engineering and Design Laboratory, ETH Zurich, 1998.

[4] A. Chiba, D. T. Power and M.A. Rahman, "Characteristics of a Bearingless Induction Motor", *IEEE Trans. Magn.*, vol. 27, pp. 5199-5201, Nov. 1991.

[5] Iwaki Pumps: http://www.iwakipumps.jp.

[6] Schmitt Kreiselpumpen: http://www.schmitt-pumpen.de.

[7] March Pumps: http://www.marchpump.com.

[8] Levitronix Pumps: http://www.levitronix.com.

[9] J. Lindström, "Thermal Model of a Permanent-Magnet Motor for a Hybrid Electric Vehicle", Internal Report, Chalmers University of Technology, Goteborg, Sweden, April 1999.

[10] C. Roulaud, "Reduced models for temperature control of a power drive with variable cooling fluid flow", *32nd Annual Conference of the IEEE Industrial Electronics Society (IECON)*, Nov. 7-10, 2006, Paris, France, pp. 4806-4812.

[11] J. Lienhard, *A Heat Transfer Textbook*, 3rd ed. Cambridge, Massachusetts, U.S.A.: Phlogiston Press, 2006.

[12] D. A. Staton, "Convection Heat Transfer and Flow Calculations Suitable for Analytical Modeling of Electric Machines", *32nd Annual Conference of the IEEE Industrial Electronics Society (IECON)*, Nov. 7-10, 2006, Paris, France, pp. 4841-4846.

[13] C. Pfeiderer, H. Petermann, *Strömungsmaschi-nen*, 6. Auflage, Berlin: Springer, 1990.

[14] Sulzer Pumps, *Sulzer Centrifugal Pump Handbook,* 2nd ed. Oxford, UK: Elsevier Advanced Technology, 1998.

[15] K. C. Wilson, *Slurry Transport Using Centrifugal Pump*, 2nd ed.: Springer, 1996.

[16] I. J. Karassik, *Pump Handbook*, 3rd ed.: McGraw-Hill, 2000.

[17] V. S. Lobanoff, *Centrifugal Pumps: Design and Application*, Gulf Professional Publishing.

[18] B. K. Gandhi, "Effect of Speed on the Performance Characteristics of a Centrifugal Slurry Pump", *J. Hydr. Engrg.*, vol. 128, Issue 2, pp. 225-233, Feb. 2002.

[19] D. Lin, "A Dynamic Core Loss Model for Soft Ferromagnetic and Power Ferrite Materials in Transient Finite Element Analysis", *IEEE Transactions on Magnetics,* vol. 40, No. 2, March 2004.

[20] M. Neff, „Magnetgelagertes Pumpsystem für die Halbleiterfertigung", Ph.D. Dissertation, Electrical Engineering and Design Laboratory, ETH Zurich, 2003.

[21] C. Heck, *Magnetische Werkstoffe und ihre technische Anwendung*, 2. Auflage, Heidelberg: Hüthig, 1975.